Throughput of Turbo Coded Hybrid ARQ Using Single-carrier MIMO Multiplexing

Akinori Nakajima, Deepshikha Garg, and Fumiyuki Adachi
Dept. of Electrical and Communications Engineering
Tohoku University, Sendai, Japan
nakajima@mobile.ecei.tohoku.ac.jp

Abstract— **Broadband wireless packet access will be the core technology of the next generation mobile communications systems. Very high speed and high quality packet transmissions can be achieved by the joint use of multiple-input multiple-output (MIMO) multiplexing and hybrid ARQ (HARQ). However, if single-carrier (SC) transmission is used, the throughput performance significantly degrades due to large inter-symbol interference (ISI) resulting from severe frequency-selective channel. Recently, we proposed an iterative parallel interference cancellation (PIC) for MIMO multiplexing in a frequency non-selective fading channel. In this paper, we propose a frequency-domain iterative PIC for SC-MIMO multiplexing to separate signals transmitted from different antennas while achieving frequency and antenna diversity gain and evaluate, by computer simulation, the throughput performance of turbo coded HARQ using SC-MIMO multiplexing in a frequency-selective Rayleigh fading channel.**

Keywords- ***SC-MIMO multiplexing, Frequency-domain Iterative PIC, Turbo coded Hybrid ARQ, FDE***

I. INTRODUCTION

Recently, there have been tremendous demands for high-speed data transmissions in mobile communications [1]. However, for such high-speed data transmissions, the channel consists of many propagation paths with different time delays, resulting in a frequency-selective fading channel. The performance of SC transmission significantly degrades due to severe inter-symbol interference (ISI) [2]. Recently, it has been shown that the use of frequency-domain equalization (FDE) can significantly improve the SC transmission performance [3,4].

However, the available bandwidth is limited, so higher spectrum efficiency is required. One of the promising techniques is the multiple-input multiple-output (MIMO) multiplexing [5-9] that uses multiple transmit and receive antennas. In MIMO multiplexing, transmit data sequence is transformed into parallel sequences and each sequence is transmitted from a different transmit antenna at the same time with the same carrier frequency. Therefore, the total transmission rate increases in proportion to the number of transmit antennas without requiring additional bandwidth.. At the receiver, it is necessary to separate the transmit signals. A lot of research attention is given to find the separation methods which provide a performance close to that of maximum likelihood detection (MLD) but with reduced complexity, like Vertical-bell laboratories layered space-time architecture (V-BLAST) [7], MLD using QR decomposition [8] and so on. Recently, we proposed an iterative parallel interference cancellation (PIC) for MIMO multiplexing in a frequency non-selective fading channel [9]. In this paper, we propose a frequency-domain iterative PIC for SC-MIMO multiplexing to separate signals transmitted from different antennas while achieving frequency and antenna diversity gain.

Broadband wireless packet access will be the core technology of the next generation mobile communications systems. Important techniques for achieving very high speed packet transmissions in a bandwidth-limited and frequency-selective channel are MIMO multiplexing and hybrid automatic repeat request (HARQ). In this paper, we consider SC-MIMO multiplexing using frequency-domain iterative PIC and evaluate, by the computer simulation, the bit error rate (BER) performance and the throughput performance of HARQ combined with rate compatible punctured turbo (RCPT) code [10] in a frequency-selective Rayleigh fading channel.

The remainder of this paper is organized as follows. Section II describes the SC-MIMO multiplexing with the frequency-domain iterative PIC. Section III presents the computer simulated performances of frequency-domain iterative PIC in a frequency-selective Rayleigh fading channel. Section IV concludes the paper.

II. FREQUENCY-DOMAIN ITERATIVE PIC FOR HARQ USING SC-MIMO MULTIPLEXING

A. Transmit and receive signal

Fig.1 shows the transmitter/receiver structure of SC-(N_t,N_r)MIMO multiplexing using frequency-domain iterative PIC. N_t transmit antennas and N_r receive antennas are used. At the transmitter, turbo coding is performed on the CRC coded binary information sequence, and the transmit sequences obtained by puncturing the turbo coded sequence are stored in the buffer. In this paper, type II HARQ S-P2 [11] is considered.

After bit-interleaving and data-modulation, the data-modulated symbol sequence is serial-to-parallel (S/P) converted to N_t parallel sequences, each to be transmitted from a different transmit antenna. In this paper, QPSK data-modulation is considered. Each QPSK modulated symbol sequence is divided into a sequence of blocks of N_c symbols each. Data symbol vector at time t is denoted by

$\mathbf{d}(t) = [d_0(t), \cdots, d_{N_t-1}(t)]^T$, where t=0~N_c-1. As shown in Fig.2, the last N_g symbols in each block is copied and inserted as a cyclic prefix into the guard interval (GI) placed at the beginning of each block to form a frame with N_g+N_c symbols. The resultant GI-inserted data symbol vector $\overline{\mathbf{d}}(t)$ to be transmitted from N_t antennas at time t, where t=-N_g~N_c-1, is expressed using the equivalent baseband representation as

$$\overline{\mathbf{d}}(t) = \sqrt{2S}\mathbf{d}(t \bmod N_c) \text{ , (1)}$$

where S is the transmit signal power per antenna.

N_t frames are transmitted simultaneously from N_t transmit antennas using the same carrier frequency. At the receiver, a superposition of N_t transmitted signals is received by N_r antennas via a frequency-selective fading channel. The channel is assumed to be a symbol-spaced L-path frequency-selective fading channel, each discrete propagation path being subjected to independent fading. It is assumed that the time delay of the lth path, l=0~L-1, is τ_l symbols with $\tau_0 = 0$ and $\tau_0 < \tau_1 < \tau_2 \cdots < \tau_{L-1}$ without loss of generality and that the GI length, N_g, is larger than τ_{L-1} . After removal of GI from the received signal, N_c-point fast Fourier transform (FFT) is applied to obtain the N_c frequency components. The received signal component vector $\mathbf{R}(k) = [R_0(k), \cdots, R_{N_r-1}(k)]^T$ of N_r receive antennas at the kth frequency can be expressed as follows:

$$\mathbf{R}(k) = \sqrt{2S}\mathbf{H}(k)\mathbf{D}(k) + \mathbf{\Pi}(k) \text{ , (2)}$$

where $\mathbf{H}(k)$, $\mathbf{S}(k)$ and $\mathbf{\Pi}(k)$ are N_r-by-N_t complex channel gain matrix, N_t-by-1 transmit symbol vector and N_r-by-1 noise vector at the kth frequency, respectively. They are given by

$$\begin{cases} \mathbf{H}(k) = \sum_{l=0}^{L-1} \mathbf{h}_l(t) \exp(-j2\pi\tau_l k / N_c) \\ \mathbf{D}(k) = \sum_{t=0}^{N_c-1} \mathbf{d}(t) \exp(-j2\pi t k / N_c) \\ \mathbf{\Pi}(k) = \sum_{t=0}^{N_c-1} \mathbf{n}(t) \exp(-j2\pi t k / N_c) \end{cases} \text{ , (3)}$$

where $\mathbf{h}_l(t)$ is the N_r-by-N_t complex path gain matrix of the lth path, given by

$$\mathbf{h}_l(t) = \begin{bmatrix} h_{0\_0,l}(t) & \cdots & h_{0\_N_t-1,l}(t) \\ \vdots & \ddots & \vdots \\ h_{N_r-1\_0,l}(t) & \cdots & h_{N_r-1\_N_t-1,l}(t) \end{bmatrix} \text{ , (4)}$$

where $h_{n_r\_n_t,l}(t)$ denotes the path gain of the lth path between the n_rth received antenna and n_tth transmit antenna. In this paper, block fading where the path gains stay constant over at least one data frame and $\sum_{l=0}^{L-1} E[|h_{n_r\_n_t,l}(t)|^2] = 1$ for all n_r and n_t are assumed. $\mathbf{n}(t) = [n_0(t), \cdots, n_{N_r-1}(t)]^T$ is the noise vector received on N_r receive antennas, where $\{ n_{n_r}(t)$; n_r=0~N_r-1$\}$ are characterized by independent zero-mean complex Gaussian processes having variance $2N_0/T$; N_0 is the one-sided power spectrum density of additive white Gaussian noise (AWGN) and T is the length of the symbol transmitted from each transmit antenna.

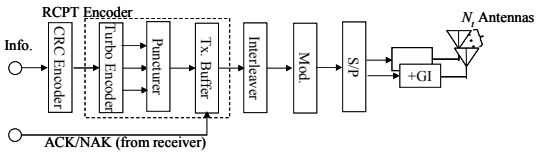

(a) Transmitter

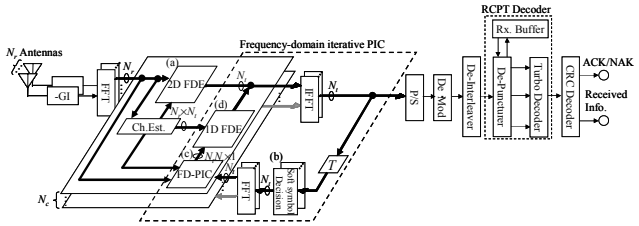

(b) Receiver

Figure 1 Transmitter/receiver structure of SC-(N_t,N_r)MIMO multiplexing using frequency-domain iterative PIC.

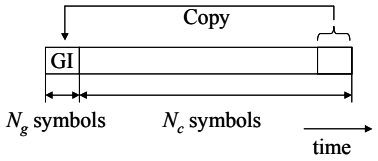

Figure 2 Frame structure.

B. Frequency-domain iterative PIC

Fig. 3 shows the operation of the frequency-domain iterative PIC. FDE based on two-dimensional (2D) minimum mean square error (MMSE) criterion is used to suppress the ISI and the interference from other transmit signals, but interference suppression is not sufficient. So, we propose to perform FDE and cancellation in an iterative fashion. The received signal vector at the kth frequency obtained by performing FDE in the ith iteration is denoted by $\widetilde{\mathbf{R}}^{(i)}(k) = [\widetilde{R}_0^{(i)}(k), \cdots, \widetilde{R}_{N_t-1}^{(i)}(k)]^T$. FDE requires accurate channel estimation. In this paper, ideal channel estimation is assumed.

(a) 2D-FDE (i=0)

For the i=0th iteration, 2D-FDE is performed to obtain $\widetilde{\mathbf{R}}^{(0)}(k)$, which can be expressed as

$$\widetilde{\mathbf{R}}^{(0)}(k) = \mathbf{W}^{(0)}(k)\mathbf{R}(k) \text{ , (5)}$$

where $\mathbf{W}^{(0)}(k)$ is the N_t-by-N_r MMSE weight matrix and is given by [2]

$$\mathbf{W}^{(0)}(k) = \mathbf{H}^H(k)[\mathbf{H}(k)\mathbf{H}^H(k) + (\sigma^2 / S)\mathbf{I}]^{-1} \text{ , (6)}$$

where $(.)^H$ is Hermit transpose operation, and $\mathbf{I}$ is the N_r-by-N_r identity matrix.

(b) Replica generation

After carrying out the ith FDE, the N_c-point IFFT is performed on $\widetilde{\mathbf{R}}^{(i)}(k)$ to obtain the time-domain decision variable $\widetilde{\mathbf{r}}^{(i)}(t)=[\widetilde{r}_0^{(i)}(t),\cdots,\widetilde{r}_{N_r-1}^{(i)}(t)]^T$ associated with the transmit symbol vector $\mathbf{d}(t)$:

$$\widetilde{\mathbf{r}}^{(i)}(t)=(1/N_c)\sum_{k=0}^{N_c-1}\widetilde{\mathbf{R}}^{(i)}(k)\exp(j2\pi tk/N_c)\,. \quad (7)$$

Then, the soft decision is carried out using $\widetilde{\mathbf{r}}^{(i)}(t)$ to generate the symbol replica $\hat{\mathbf{d}}^{(i+1)}(t)=[\hat{d}_0^{(i+1)}(t),\cdots,\hat{d}_{N_t-1}^{(i+1)}(t)]^T$ to be used in the (i+1)th iteration. The symbol replica $\hat{d}_{n_t}^{(i+1)}(t)$ transmitted from the n_tth antenna is generated by using $\widetilde{r}_{n_t}^{(i)}(t)$ as follows:

$$\hat{d}_{n_t}^{(i+1)}(t)=\frac{1}{\sqrt{2}}\tanh(\beta\frac{\mathrm{Re}[\widetilde{r}_{n_t}^{(i)}(t)]}{\sqrt{2S}})+j\frac{1}{\sqrt{2}}\tanh(\beta\frac{\mathrm{Im}[\widetilde{r}_{n_t}^{(i)}(t)]}{\sqrt{2S}}) \quad , (8)$$

where β is a parameter that controls the extent to which the soft value contributes to the replica generation.

(c) PIC operation

After performing soft decision, FFT is carried out using $\hat{\mathbf{d}}^{(i+1)}(t)$ to obtain the frequency-domain signals $\hat{\mathbf{D}}^{(i+1)}(k)=[\hat{D}_0^{(i+1)}(k),\cdots,\hat{D}_{N_t-1}^{(i+1)}(k)]^T$:

$$\hat{\mathbf{D}}^{(i+1)}(k)=\sum_{t=0}^{N_c-1}\hat{\mathbf{d}}^{(i+1)}(t)\exp(-j2\pi kt/N_c)\,. \quad (9)$$

The interference replicas $\sqrt{2S}\mathbf{H}(k)\hat{\mathbf{D}}^{(i+1)}(k)$ are generated and then, subtracted from the received signals to obtain the N_tN_r-by-1 received signal vector $\hat{\mathbf{R}}^{(i+1)}(k)=[\hat{\mathbf{R}}_0^{(i+1)}(k),\cdots,\hat{\mathbf{R}}_{N_t-1}^{(i+1)}(k)]^T$, where the n_tth component vector $\hat{\mathbf{R}}_{n_t}^{(i+1)}(k)=[\hat{R}_{0\_n_t}^{(i+1)}(k),\cdots,\hat{R}_{N_r-1\_n_t}^{(i+1)}(k)]$ corresponds to the N_r-by-1 received symbol vector transmitted from the n_tth antenna. The PIC operation to extract the received signal component vector $\hat{\mathbf{R}}_{n_t}^{(i+1)}(k)$ is expressed as

$$\hat{\mathbf{R}}_{n_t}^{(i+1)}(k)=\mathbf{R}(k)-\sqrt{2S}\{\mathbf{H}(k)\hat{\mathbf{D}}^{(i+1)}(k)-\mathbf{H}_{n_t}(k)\hat{D}_{n_t}^{(i+1)}(k)\} \quad , (10)$$

where $\mathbf{H}_{n_t}(k)$ is the N_r-by-1 channel gain vector (the n_tth component vector of $\mathbf{H}(k)$) between the n_tth transmit antenna and N_r receive antennas.

(d) 1D-FDE (i>0)

Since ISI can be partially removed from the received signals by performing PIC, the resulting signals are close to the case of single antenna transmissions. Hence, one-dimensional (1D) MMSE-FDE is applied, for i>0. Joint 1D-FDE and antenna diversity combining is performed to obtain the signal component $\widetilde{\mathbf{R}}^{(i+1)}(k)$ at the kth frequency as

$$\widetilde{\mathbf{R}}^{(i+1)}(k)=\mathbf{W}^{(i+1)}(k)\hat{\mathbf{R}}^{(i+1)}(k)\,, \quad (11)$$

where $\mathbf{W}^{(i+1)}(k)$ is the N_t-by-N_tN_r MMSE equalization weight matrix at the (i+1)th iteration, and is given by

$$\mathbf{W}^{(i+1)}(k)=diag[\mathbf{W}_0^{(i+1)}(k),\cdots,\mathbf{W}_{N_t-1}^{(i+1)}(k)]\,, \quad (12)$$

where [4]

$$\mathbf{W}_{n_t}^{(i+1)}(k)=\mathbf{H}_{n_t}^H(k)[\mathbf{H}_{n_t}^H(k)\mathbf{H}_{n_t}(k)+(\sigma^2/S)^{-1}]^{-1}\,. \quad (13)$$

Here, $\mathbf{W}_{n_t}^{(i+1)}(k)$ is the n_tth row component vector of $\mathbf{W}^{(i+1)}(k)$.

The above processes (b)~(d) are repeated sufficient number of times. Then, N_t transmitted symbol frames are recovered and converted into serial symbol sequence by P/S conversion for data-demodulation and RCPT decoding. In the RCPT decoder, de-puncturing, turbo decoding, and error detection are performed. The result of error detection is transmitted to the transmitter as ACK/NACK.

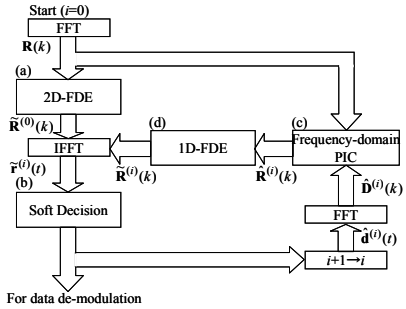

Figure 3 Operation of frequency-domain iterative PIC.

III. RCPT HARQ

Fig.4 shows transmit packet generation method of RCPT Type II HARQ. In this paper, turbo encoder of coding rate R=1/3 is applied. The turbo encoder outputs the systematic bit (information bit) sequence and two parity bit sequences, each has length of K bits. These bit sequences' is K. In this paper, we consider RCPT HARQ S-P2 [11]. It is explained in detail as follows. At the transmitter, the first packet consisting of systematic bits is transmitted. At the receiver, error detection is performed. If there are errors in the received packet, an NACK is transmitted to the transmitter. Then, the second packet is transmitted. It is punctured one of the two parity bit sequences generated with puncture period P=2. Puncturing pattern can be expressed as follows:

$$\begin{bmatrix}1&1\\0&0\\0&0\end{bmatrix}\quad\begin{bmatrix}0&0\\1&0\\0&1\end{bmatrix}\quad\begin{bmatrix}0&0\\0&1\\1&0\end{bmatrix}\,. \quad (14)$$

At the receiver, depuncturing is performed followed by turbo decoding. The parity bits which have not been received yet are replaced by a channel value 0. In this case, turbo decoding corresponds to R=1/2. After turbo decoding, the error detection is performed. If error is detected, the receiver transmits the NACK again. At the transmitter, another punctured parity bit sequence is transmitted. In the receiver side, the second and third received packets are transformed into two parity bit sequences by depuncturing and then, R=1/3 turbo decoding is carried out again.

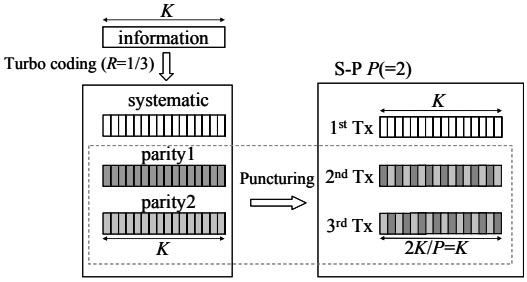

Figure 4 Transmit packet generation for RCPT Type II HARQ S-P2.

IV. COMPUTER SIMULATION

We assume an information bit sequence of K=2048 bits. Coding rate R=1/3 turbo encoder consisting of two (7,5) recursive systematic convolutional (RSC) encoders [12] is employed. We assume that N_r-by-N_t channels are independent and identically distributed frequency-selective Rayleigh fading channels and have symbol-spaced exponentially decaying L=16-path power delay profile with decay factor α. Block fading and ideal channel estimation are assumed as in Sect. III.

Table 1. Simulation conditions

Transmitter	Data Modulation	QPSK
	Number of Tx Antennas	N_t=2,4
	Number of FFT points	N_c=256
	GI	N_g=32
Channel	Frequency-selective block Rayleigh fading	
	Power delay profile	L=16-path exponential power delay profile
		Decay factor α=0dB
Receiver	Channel estimation	Ideal
	Number of Rx Antennas	N_r=2,4

Fig.5 plots the average BER of SC-(2,2)MIMO multiplexing as a function of β. Average signal energy per information bit-to-AWGN power spectrum density ratio E_b/N_0 per receive antenna is set as 6dB. It can be seen that the average BER is not so sensitive to β for $\beta \geq 5$, however the optimum value is seen to be about β=5. In the following simulations, we use β=5.

Fig.6 plots the uncoded BER performance of SC-(2,2)MIMO multiplexing as a function of the average received E_b/N_0. It can be seen that the BER performance improves with the increase in the number of iterations. However, the use of 4 iterations is sufficient since the additional improvement becomes smaller as the number of iterations increases. For comparison, the result for perfect PIC (i.e., the interference from the other antennas are cancelled perfectly) is also plotted. The loss in the required average received E_b/N_0 from perfect PIC for an average BER=10^{-4} reduces to about 0.4 dB at i=4.

Fig.7 plots the RCPT HARQ throughput performance of the SC-(N_t,N_r)MIMO multiplexing as a function of the average received energy per symbol-to-noise power spectrum density ratio E_s/N_0 per receive antenna. When (N_t,N_r)=(2,2) and (4,4), the throughput with i=4 is, at most, about 1.9 and 2.0 times as good as that without iterations, respectively, and close to that of perfect PIC. For comparison, the throughput of SC-(1,2) and (1,4)SIMO corresponding to single antenna transmission is also plotted. For E_s/N_0>3dB, the performance of SC-(2,2)MIMO with i=4 is, at most, about 2 times better than that of SC-(1,2)SIMO. On the other hand, the performance of SC-(4,4)MIMO with i=4 is about 4 times better than that of SC-(1,4)SIMO for E_s/N_0>9dB.

Fig.8 plots the throughput performances of SC-(N_t,N_r)MIMO multiplexing and OFDM-(N_t,N_r)MIMO multiplexing. In OFDM-MIMO multiplexing, log likelihood ratio (LLR) [13] is applied to each sub-carrier as a separation method. LLR corresponds to the soft output of MLD. It can be seen from this figure that the performance of SC-MIMO multiplexing is superior to that of OFDM-MIMO multiplexing. When (N_t,N_r)=(2,2) and (4,4), the performance of SC-MIMO multiplexing is 1.0~1.9 and 1.0~1.7 times as good as that of OFDM-MIMO multiplexing, respectively. This reason is explained as follows. OFDM has no diversity gain without channel coding. Since no parity bits are transmitted with the first transmission, a second transmission is almost always requested to benefit from coding gain. However, for SC system, there is a large frequency diversity gain even without channel coding. For large E_s/N_0, retransmission may not be necessary and thus has a higher throughput.

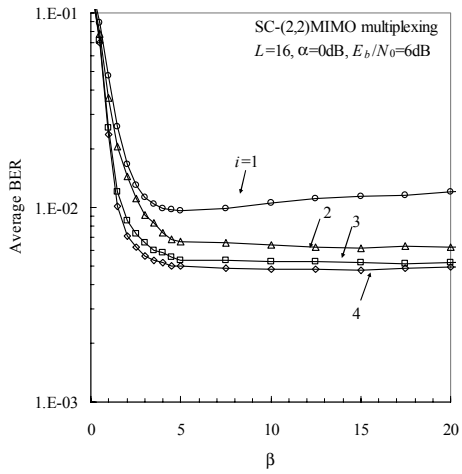

Figure 5 Impact of the parameter β on average BER

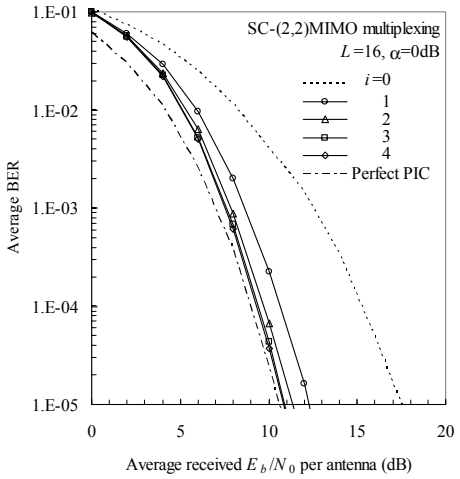

Figure 6 Uncoded BER performance.

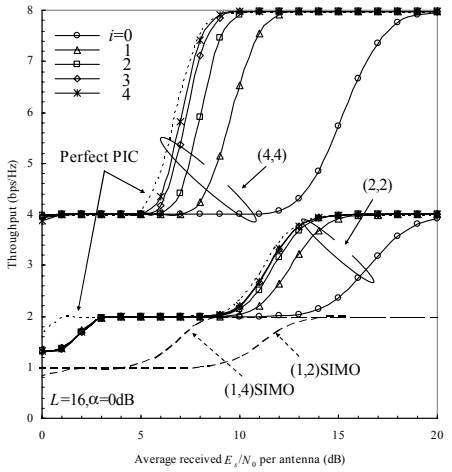

Figure 7 Effect of frequency-domain iterative PIC.

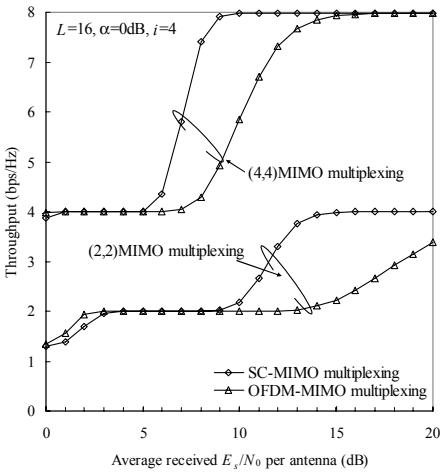

Figure 8 Throughput comparison between SC-MIMO multiplexing and OFDM-MIMO multiplexing

V. CONCLUSIONS

In this paper, we proposed a frequency-domain iterative PIC scheme for SC-MIMO multiplexing to separate signals transmitted from different antennas while achieving frequency and antenna diversity gain. We evaluated, by computer simulation, the BER and throughput performance of SC-MIMO multiplexing with frequency-domain iterative PIC in a frequency-selective Rayleigh fading channel.

It was found that the use of 4 iterations is enough for performance improvement; the BER performance loss with 4 iterations from ideal PIC is as small as 0.4dB at BER=10^{-4} and the throughput performance with 4 iterations is better by about 1.9 and 2.0 times, at most, than that without iterations when (N_t,N_r)=(2,2) and (4,4), respectively. In addition, the throughput of SC-MIMO multiplexing was compared with that of OFDM-MIMO multiplexing to show the performance of SC-MIMO multiplexing is superior as it benefits from a large frequency diversity gain.

REFERENCES

[1] F. Adachi, "Wireless past and future-evolving mobile communications systems," IEICE Trans. Fundamentals, vol.E84-A, pp.55-60, Jan. 2001.

[2] John G. Proakis, *Digital Communications*, 4th edition, McGraw-Hill, 2001.

[3] D. Falconer, et al., "Frequency domain equalization for single-carrier broadband wireless systems," IEEE Commun. Mag., vol.40, pp.58-66, April 2002.

[4] K. Takeda, T. Itagaki, and F. Adachi, "Joint use of frequency-domain equalization and transmit/receive antenna diversity for single-carrier transmissions," IEICE Trans. Commun., vol. E87-B, no.7, pp.1946-1953, July 2004.

[5] G. J. Foschini and M. J. Gans, "On Limits of wireless communications in a fading environment when using multiple antennas," Wireless Personal Commun., vol.6, no. 3, pp. 311-335, 1998.

[6] R. van Nee, A. van Zelst, and G. Awater, "Maximum likelihood decoding in a space division multiplexing system," Proc. IEEE VTC 2000-Spring, vol.1, pp.6-10, May 2000.

[7] P. W. Wolniansky, et al., "V-BLAST: an architecture for realizing very high data rates over the rich-scattering wireless channel," Proc. ISSSE, pp.295-300, Sept. 1998.

[8] H. Kawai, et al., "Likelihood function for QRM-MLD suitable for soft-decision turbo decoding and its performance for OFCDM MIMO multiplexing in multipath fading channel," IEICE Trans. Commun., vol E88-B, no.1, pp.47-57, Jan. 2005.

[9] A. Nakajima, et al., "Iterative adaptive soft parallel interference canceller for turbo coded MIMO multiplexing," IEICE Trans. Commun., vol E87-B, no.12, pp.3813-3819, Dec. 2004.

[10] D. N. Rowitch and L. B. Milstein, "Rate compatible punctured turbo (RCPT) codes in hybrid FEC/ARQ system," Proc. Comm. Theory Mini-conference of GLOBECOM'97, pp. 55-59, Nov. 1997.

[11] D. Garg and F. Adachi, "Rate compatible punctured turbo-coded hybrid ARQ for OFDM in a frequency selective fading channel," Proc. IEEE VTC2003-Spring, pp.2725-2729, Jeju, Korea, April 2003.

[12] J. P. Woodard and L. Hanzo, "Comparative study of turbo decoding techniques: an overview," IEEE Trans. Veh. Technol., vol.49, no.6, pp. 2208-2233, Nov. 2000.

[13] A. Stefanov and T. M. Duman, "Turbo coded modulation for wireless communications with antenna diversity," IEEE Journal on Sel. Areas in Comm., vol. 19, pp. 958-968, May 2001.